Macromolecules **2008**, *41*, 7687−7694

Investigation of the Assembly of Comb Block Copolymers in the Solid State

M. Brett Runge,[†] Corinne E. Lipscomb,[‡] Lindsay R. Ditzler,[†] Mahesh K. Mahanthappa,[‡] Alexei V. Tivanski,[†] and Ned B. Bowden*,[†]

Department of Chemistry, University of Iowa, Iowa City, Iowa 52242, and Department of Chemistry, University of Wisconsin at Madison, 1101 University Ave., Madison, Wisconsin 53706

Received April 25, 2008; Revised Manuscript Received August 22, 2008

ABSTRACT: Comb block copolymers are a relatively new architecture of polymer whose assembly into ordered morphologies in the solid state is largely unexplored. Thirty-two comb block copolymers with molecular weights from 168 to 4200 kg mol^{-1} were synthesized and assembled in the solid state into ordered morphologies with domain sizes as large as 138 nm. The individual structures of these polymers were studied by atomic force microscopy and scanning electron microscopy to identify their shapes. The solid-state morphologies of these polymers were imaged by scanning electron microscopy and small-angle X-ray scattering when permissible. Four phase maps were plotted from the 32 data points generated in this work to investigate how differences in polymer compositions affected the final morphologies. A clear relationship between the compositions of polymers and their morphologies was observed. The polymers were systematically altered to investigate the relationship between their compositions and the domain sizes of their morphologies. In one set of samples, the molecular weights of the arms were kept constant while the molecular weight of the backbone polymer was increased. In a second set of examples, the backbone polymer remained constant while the molecular weights of the arms were increased. While higher molecular weight polymers generally led to larger domain spacings in the microphase-separated structures, variations in the comb arm lengths resulted in dramatic changes in the observed solid-state morphologies. This paper is the first to provide a detailed study of a large series of comb block copolymers to relate their compositions to their assembled morphologies in the solid state.

Introduction

The assembly of block copolymers into ordered materials in the solid state with domain sizes with nanoscopic dimensions is important for many applications ranging from new lithographic methods for microchip manufacture to photonic materials.[1−7] The microphase separation of block copolymer soft materials into a variety of one-, two-, and three-dimensionally ordered morphologies offers opportunities to template nanomaterials that are challenging, if not impossible, to fabricate by other methods.[5,6,8−25] This approach is attractive because robust synthetic methods in polymer chemistry offer the ability to synthesize self-assembling block copolymers having well-defined compositions, structures, and placement of reactive functional groups within or surrounding templated nanostructures. These features of block copolymer microphase separation provide unique opportunities for the "bottom-up" fabrication of structurally and chemically uniform nanomaterials that may exhibit new materials properties. For example, linear block copolymers have been shown to adopt ordered morphologies in thin films that render them useful for patterning surfaces with feature sizes ranging from 5 to 90 nm.[24,25,42] Because their assembly is well understood both experimentally and theoretically, these polymers provide a basis for understanding how more complex polymers assemble in the solid state. In order to achieve larger domain spacings and, thus, larger template dimensions, these polymers can be swelled with various additives that also introduce defects.[4,26−34] Applications of these swelled nanomaterials are limited because of the presence of these defects.

The field of assembling block copolymers has become increasingly complex due to advances in polymerization techniques that allow the synthesis of new polymers with different, complex architectures including multiblock, miktoarm star, and comb polymers.[35−41] Although these new architectures of polymers may have applications in drug delivery, catalyst immobilization, and photonic materials, the self-assembly of these polymers in the solid state is poorly understood.[34,42−49] Recent work has shown that thin films of these materials exhibit complex morphologies and unusually large domain spacings. For example, some rod−coil polymers assemble in the solid state to form morphologies with domain sizes that readily exceed 100 nm. This result is remarkable because these rod−coil polymers have modest molecular weights, but only the highest molecular weight linear polymers have morphologies with domain sizes in this size range.[50]

Recently, we reported the synthesis of and the first examples of ordered morphologies in a new large block copolymer: comb block copolymers.[51] This new architecture of block copolymer possesses a few critical attributes that make it distinctly different from a linear block copolymer such that its assembly is unique. Comb block copolymers possess different conformations than linear block copolymers because one block is decorated with polymeric arms (Figure 1). The block with the polymeric arms assumes either a globular shape based on a random coil or a rigid rod depending on the level of steric crowding between the polymeric arms that may result in elongation of the backbone polymer.[26,51−68] Regardless of the shape of these polymers, the polymeric arms will mostly or completely encapsulate the block on the backbone polymer to which they are bonded to ease steric crowding. As a consequence of the polymer architecture, backbone polymers with moderate degrees of polymerization result in comb block copolymers that possess high molecular weights measured in hundred of thousands to millions of grams per mole. In our prior work, we demonstrated that these polymers assemble in the solid state into ordered morphologies with domain sizes that may exceed 200 nm.[51,62] Our values were

---

* To whom correspondence should be addressed: e-mail ned-bowden@uiowa.edu; Fax (319) 335-1270.

[†] University of Iowa.

[‡] University of Wisconsin at Madison.

10.1021/ma8009323 CCC: $40.75

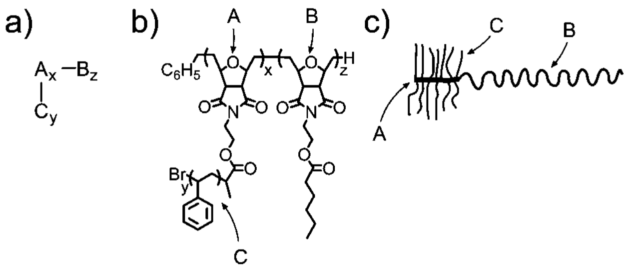

Figure 1. (a) Comb block copolymers can be viewed as C−A−B triblock polymers. (b) Chemical structures of a comb block copolymer that emphasizes which block is labeled as A, B, or C. (c) Schematic representation of a comb block copolymer to emphasize the placement of the arms along one block of the backbone polymer.

the largest domain sizes observed for block copolymers assembled in the absence of additives.

Although comb block copolymers may possess molecular weights measured in the millions of grams per mole, they assemble in the solid state into ordered morphologies. These comb block copolymers can be viewed as either triblock copolymers—they certainly possess three blocks—or as diblock copolymers because the arms encapsulate the section of the backbone to which they are bonded. In the latter case, comb block copolymers can be viewed as similar to diblock copolymers with one block due to one section of the backbone polymer (B in Figure 1) and a second block due to a combination of the arms and the section of the backbone polymer to which they are bonded (A and C in Figure 1). Whether these polymers assemble into morphologies commonly seen for triblock or diblock polymers is one of the questions that will be addressed in this paper. Here, we investigate the assembly of 32 comb block copolymers to demonstrate how to predict morphologies and domain sizes from their chemical compositions.

Many different parameters that affect the assembly of comb block copolymers are examined. For instance, the molecular weight of the arms, molecular weight of the backbone polymer, overall polymer composition, and overall molecular weight of the comb polymer affect both the morphologies and domain sizes of assemblies of these polymers in the solid state. Each of these parameters was studied to identify and to control the factors that lead to their assembly in the solid state. The assembled arrays were characterized by scanning electron microscopy (SEM) and confirmed by small-angle X-ray scattering (SAXS) when possible. Four different phase maps were generated in order to investigate which characteristics of comb polymers control the formation of each morphology. In these phase maps, the volume fraction of the respective blocks, degrees of polymerization, and backbone composition are used to show how they affect the assemblies of comb block copolymers. This work represents a critical first step in the understanding of this important polymer architecture that may extend some of the potential applications of block copolymers.

Experimental Section

Synthesis and Characterization of Asymmetric Comb Block Copolymers. The synthesis of comb block copolymers is shown in Figure 2. The full procedure for their synthesis and characterization was reported in two earlier publications and will not be repeated in detail here.[51,62] Several important characterization methods that were used to confirm the compositions and molecular weights deserve a brief description because of the size and complexity of these polymers compared to traditional linear block copolymers. Size exclusion chromatography (SEC) equipped with refractive index and light scattering detectors were used to measure the absolute molecular weights and polydispersities of the backbone polymer, polymeric arms, and comb block copolymers without the use of linear polystyrene standards. Polymeric arms were cleaved from the comb polymer with KOH and analyzed independently of the comb polymer to confirm their molecular weights and polydispersities.

Self-Assembly and Characterization of Assembled Polymers. The polymer films were assembled by first casting polymer films from methylene chloride by evaporation onto glass slides or silicon wafers. Typical concentrations of the polymer were ~10 mg mL^{-1}. Initially these films were poorly ordered as seen by SEM, so they were vapor annealed with methylene chloride under reduced pressure. The films were placed in a Schlenk flask attached to a reservoir of methylene chloride in a separate flask. The methylene chloride was frozen with liquid nitrogen, and the flasks were evacuated. The flasks were sealed and allowed to warm to room temperature. The films were vapor annealed for 3−10 days. The polymer films were characterized by freeze fracturing to expose their interiors, followed by subsequent staining with RuO_4. They were then imaged on a Hitachi 4800 SEM at accelerating voltages of 5 kV.

SAXS. Laboratory source SAXS measurements were conducted in the Materials Science Center facility at the University of Wisconsin using a Rigaku S-MAX 3000 SAXS system. Cu Kα X-rays from a MicroMax-002+ sealed tube source were focused using a Max-Flux confocal optic followed by beam collimation through three pinhole slits to yield a final spot size of 0.9 mm at the sample. Samples were mounted in a vacuum chamber. 2D SAXS data were acquired using a Rigaku multiwire area detector with a circular active area of 133 mm with a sample-to-detector distance of 2.015 m. Typical exposure times were 120−180 s, and all data were collected at 22 °C.

Results and Discussion

Choice of Comb Block Copolymers. A diverse array of comb block copolymers was synthesized by varying the degree of polymerization of the backbone polymers and arms to investigate the important parameters that affect their assembly in the solid state. The synthesis and characterization were reported in several previous publications and will not be discussed here; rather, important aspects of the structures will be described.[51,62] The compositions and degrees of polymerizations of the backbone polymers were controlled through living ring-opening metathesis polymerizations using Grubbs' first-generation catalyst. The polymers had low polydispersities, their backbones were completely hydrogenated, and the predicted molecular weights matched the measured molecular weights to a reasonable degree of accuracy. They had degrees of polymerization that ranged from 275 to 2350 with 4 to 20% of the monomer units decorated with the ATRP initiators from which the polystyrene arms were grafted. The characterization of the backbone polymers is reported in the Supporting Information.

The polystyrene arms were synthesized by atom transfer radical polymerization (ATRP) to yield molecular weights below 10 000 g mol^{-1} per arm (Table 1). In the nomenclature, $\mathrm{M}_{x:y}\mathrm{N}_z$, followed in Table 1 x is the degree of polymerization of monomer M, y is the measured M_n of an arm of polystyrene, and z is the degree of polymerization of monomer N (see Figure 2). The molecular weights of the arms were chosen to minimize entanglement of arms between adjacent comb block copolymers.[26−29,54,57,59,69] In recent work, Inkson and McLeish expanded the Milner−McLeish model that describes the linear rheology of star polymers to describe comb polymers.[53,55] Two critical observations from their work are that comb polymers will reptate best in the solid state if the density of arms is high and their molecular weights are well below the entanglement molecular weight. Thus, we synthesized polystyrene arms with molecular weights less than the entanglement molecular weight of polystyrene (13 000 g mol^{-1}) to facilitate assembly into ordered morphologies in the solid state. In addition, a more practical concern kept the desired molecular weights of the arms

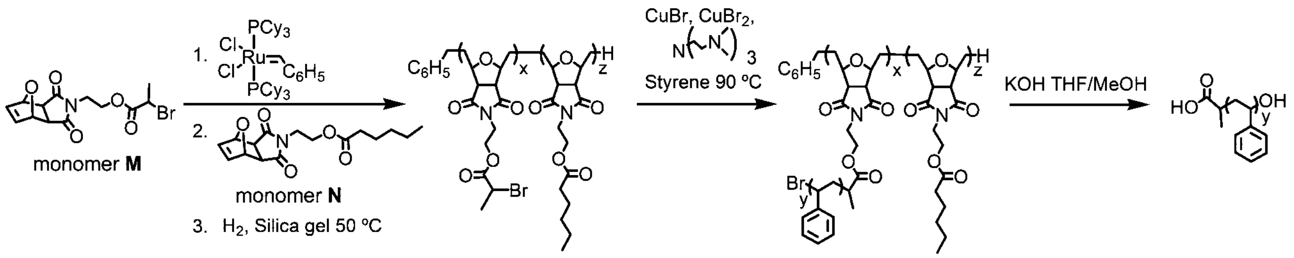

Figure 2. Synthesis of asymmetric comb block copolymers and the different polymers that were characterized by SEC to determine comb polymer composition.

Table 1. Comb Block Copolymer Characterization

entry $M_{x:y}$:N_z[a]	predicted M_n[b] (kg mol^{-1})	measured M_n (kg mol^{-1})	PDI	R_z (nm)	R_h (nm)	arms M_n[c] (g mol^{-1})	percent mol/vol fraction polystyrene[d]	percent mol/vol fraction block M[d]	percent mol/volume fraction block N[d]	morphology[e]	domain size[f] (nm)
$M_{25:3100}:N_{250}$	164	168	1.10	12.1	8.0	3100	73/0.49	2/0.05	25/0.46	C	45 ± 2
$M_{25:3500}:N_{250}$	174	262	1.14	10.4	10.4	3500	75/0.52	2/0.05	23/0.43	C	45 ± 1
$M_{25:4370}:N_{250}$	196	212	1.14	10.3	9.4	4370	79/0.58	2/0.04	19/0.38	C	48 ± 7
$M_{25:6270}:N_{250}$	243	276	1.14	10.6	10.8	6270	85/0.66	1/0.04	14/0.30	C	48 ± 2
$M_{100:3730}:N_{400}$	531	416	1.14	17.4	12.4	3730	86/0.69	2/0.07	11/0.24	C	72 ± 4
$M_{100:4180:}:N_{400}$	576	533	1.15	15.6	11.6	4180	89/0.74	2/0.06	9/0.20	S	
$M_{50:3530:}:N_{500}$	349	425	1.27	22.5	14.5	3530	76/0.52	2/0.05	22/0.43	C	65 ± 15
$M_{50:5340}:N_{500}$	439	437	1.37	31.2	15.8	5340	82/0.62	2/0.04	16/0.34	C	76 ± 4
$M_{100:1590}:N_{1000}$	503	410	1.11	26.7	16.8	1590	58/0.33	4/0.07	38/0.60	L	70 ± 4
$M_{100:3740}:N_{1000}$	718	510	1.08	19.7	13.4	3740	77/0.54	2/0.05	21/0.41	C	87 ± 12
$M_{100:4560}:N_{1000}$	800	766	1.13	26.6	18.2	4560	80/0.59	2/0.04	18/0.37	C	112 ± 11
$M_{250:3110}:N_{1000}$	1170	1290	1.25	30.5	21.0	3110	86/0.68	3/0.07	11/0.25	C	93 ± 3
$M_{250:3910}:N_{1000}$	1370	1470	1.26	35.5	26.2	3910	88/0.73	2/0.06	10/0.21	S	
$M_{150:687:}:N_{1500}$	619	551	1.27	41.5	22.7	687	37/0.19	6/0.08	57/0.73	L	85 ± 4
$M_{150:3750}:N_{1500}$	1080	947	1.15	35.1	21.3	3750	77/0.54	2/0.05	21/0.41	C	109 ± 9
$M_{150:5700}:N_{1500}$	1370	1110	1.16	34.5	21.4	5700	83/0.64	2/0.04	15/0.32	C	111 ± 17
$M_{150:5790}:N_{1500}$	1380	1040	1.13	31.3	19.9	5790	83/0.64	2/0.04	15/0.32	S	123 ± 16
$M_{150:6750}:N_{2000}$	1680	1460	1.22	40.1	23.3	6750	82/0.62	1/0.03	17/0.35	C	138 ± 15
$M_{150:4630}:N_{2000}$	1370	1200	1.13	32.9	22.0	4630	75/0.53	2/0.04	23/0.43	C	118 ± 11
$M_{150:4540}:N_{2000}$	1350	1040	1.12	37.3	22.0	4540	75/0.52	2/0.04	23/0.44	C	77 ± 3
$M_{200:1850}:N_{2000}$	1060	729	1.06	34.5	21.5	1850	62/0.37	3/0.06	35/0.57	L	98 ± 10
$M_{200:3240}:N_{2000}$	1340	1030	1.06	36.9	22.4	3240	74/0.50	2/0.05	24/0.45	C	114 ± 6
$M_{200:3620}:N_{2000}$	1410	1130	1.09	41.0	26.0	3620	76/0.53	2/0.05	22/0.42	C	126 ± 13
$M_{200:5120}:N_{2000}$	1710	1110	1.08	34.9	25.8	5120	82/0.62	2/0.04	16/0.34	C	137 ± 9
$M_{200:6410}:N_{2000}$	1970	1970	1.13	41.1	26.0	6410	85/0.67	1/0.03	14/0.30	S	
$M_{250:2120}:N_{2000}$	1240	1640	1.03	47.6	26.2	2120	69/0.45	4/0.07	27/0.48	L	116 ± 17
$M_{250:5270}:N_{2000}$	2020	3110	1.05	45.5	29.6	5270	85/0.67	2/0.04	13/0.29	S	
$M_{250:6170}:N_{2000}$	2250	2970	1.04	44.5	28.0	6170	87/0.70	1/0.04	12/0.26	S	
$M_{250:6280}:N_{2000}$	2270	3350	1.06	49.3	30.0	6280	87/0.70	1/0.04	12/0.26	S	
$M_{350:4160}:N_{2000}$	2200	1940	1.27	41.0	24.3	4160	86/0.68	2/0.05	12/0.27	S	
$M_{350:5980}:N_{2000}$	2830	3540	1.02	43.5	29.3	5980	89/0.75	2/0.04	9/0.21	S	
$M_{350:7020}:N_{2000}$	3200	4200	1.03	51.0	33.0	7020	91/0.78	1/0.04	8/0.18	S	

[a] Nomenclature used throughout this paper that describes the comb polymer backbone composition and M_n of the polystyrene arms as shown in Figure 2. [b] M_n predicted from the backbone composition and molecular weight of the polymer arms characterized after cleavage from the comb polymer. [c] Measured M_n of polystyrene arms after being cleaved from the comb polymer. [d] Calculated from moles of styrene per cleaved arm and predicted composition of backbone as described in the Supporting Information. These calculations assume bulk homopolymer densities and room temperature as described in the Supporting Information. [e] C refers to cylindrical, S to spherical, and L to lamellar morphologies. The spherical morphologies were disordered. [f] Domain sizes measured from SEM micrographs. The spherical morphologies were too disordered to find a reliable value for their domain sizes.

low. To access a reasonable range of volume fractions for each block of the comb polymer, the molecular weights of the arms had to be low such that the volume fractions of the arms ranged from 0.19 to 0.78.

These asymmetric comb block copolymers were characterized by SEC equipped with a light scattering detector to measure their absolute molecular weights. To verify their compositions and molecular weights, the arms were cleaved from the backbone by dissolving the comb polymers in a mixture of CH_2Cl_2 and MeOH with a large excess of KOH and heating at 60 °C for 24 h. The ester bonds that linked the arms to the backbone were cleaved under these conditions, and the resulting polystyrene arms were easily isolated by precipitation into MeOH. Thus, the arms were characterized independently of the comb polymers. Molecular weights for comb polymers were then calculated from the composition and molecular weight of the backbone polymer and the measured molecular weight of the arms. The measured and predicted molecular weights for comb block copolymers agreed well with each other (Table 1). Efforts to synthesize backbone polymers with degrees of polymerization larger than 2350 were successful, but these polymers were insoluble in styrene and resulted in insoluble comb polymers.

Characterization of Configurations of Single Polymers. It is important to elucidate the conformation of individual polymers to understand their self-assembly in the solid state. Individual comb polymers can assume two limiting shapes: rigid rods and random coils.[53,55−60,64,70,71] The difference in these shapes was due to steric crowding between arms decorated along the backbone polymer. If steric crowding was high, the backbone would assume a mostly linear conformation, and the comb polymer would appear as a rigid rod. Conversely, if steric

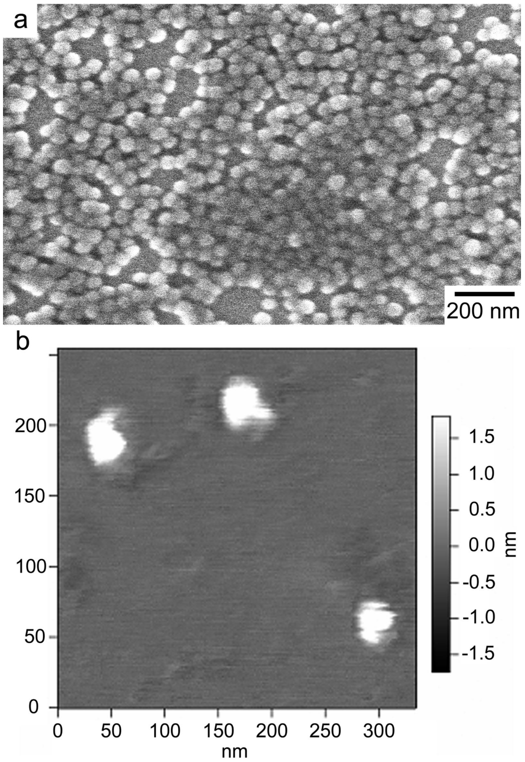

Figure 3. (a) SEM micrograph showing polymer globules of $M_{200:3240}$:N_{2000} cast on a silicon wafer from a 1 uM dioxane polymer solution. (b) AFM micrograph of $M_{200:6410}$:N_{2000} cast from methylene chloride onto mica.

crowding was low, the backbone would assume a random orientation, and the polymer would appear to be shaped as a random coil.

The shapes of these comb block copolymers were studied by light scattering, SEM, and AFM. Light scattering data of these asymmetric comb block copolymers had ratios of R_z (root-mean-square radius) to R_h (hydrodynamic radius) that varied, but most were between 1.0 and 1.5 rather than the predicted value of 2.0 for rigid-rod polymers.[72−74] These values indicate that the polymers adopted random coil configurations in solution. This result was confirmed by both SEM and AFM micrographs as shown in Figure 3. Analysis by AFM of the polymer molecules that were deposited on mica followed by evaporation of solvent indicates a size distribution with an average height of 3.9 ± 0.5 nm and diameter of 47 ± 5.2 nm. These measurements are consistent with previous results that indicate the polymers "flatten" upon removal of solvent but still maintain their overall configurations.[75]

Characterization of Morphologies of Assembled Polymers Films by SEM. As a result of the large molecular weights of our comb block copolymers, they assembled into morphologies with domain sizes of 40−138 nm. Because of these sizes, it was possible to image them by SEM rather than the more challenging transmission electron microscopy.

Many SEM micrographs are supplied in the Supporting Information, but Figures 4 and 5 show some representative examples. In Figure 4, SEM micrographs show that $M_{100:1590}$:N_{1000} assembled into a well-ordered lamellar morphology with long-range order and $M_{25:4370}$:N_{250} assembled into a cylindrical morphology with large grain sizes. To illustrate that the polymers were ordered near the surface, we show an SEM micrograph of $M_{100:4560}$:N_{1000} in Figure 5. This polymer assembled such that the long axis of the cylinders was perpendicular to the surface; however, the orientation changed as the distance from the polymer/air interface increased. These SEM micrographs provided a method to measure the domain sizes from a series of micrographs of each polymer. They form the basis for discussion of the phase maps and domain sizes in the subsequent sections.

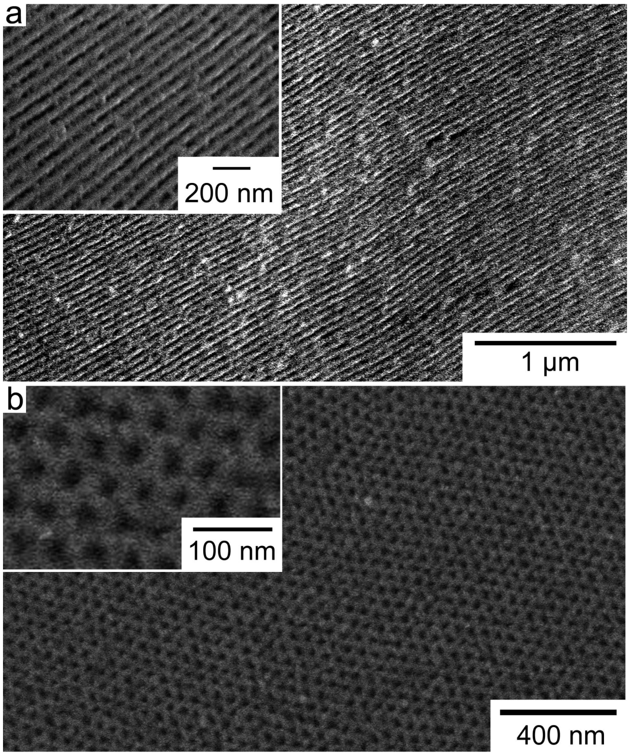

Figure 4. (a) SEM micrograph of entry $M_{100:1590}$:N_{1000} in the solid state showing a lamellar morphology. (b) SEM micrograph of entry $M_{25:4370}$:N_{250} in the solid state showing hexagonally packed cylinders.

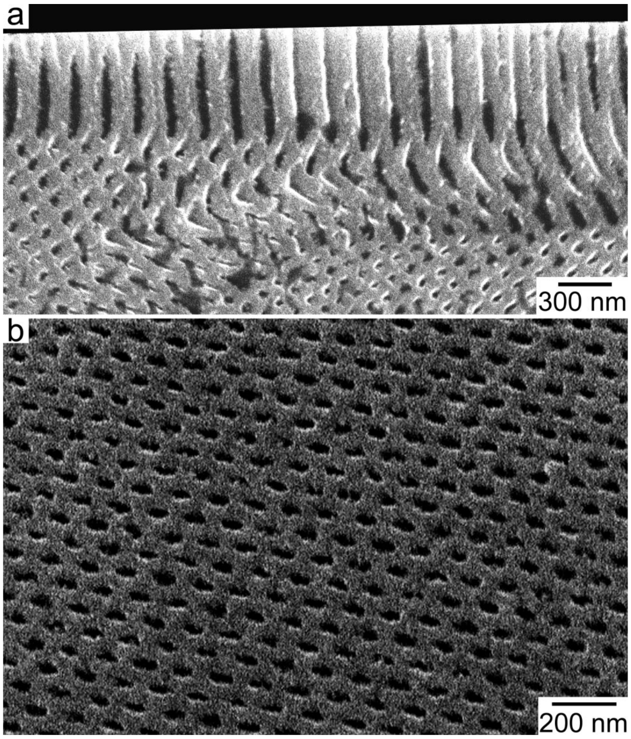

Figure 5. SEM micrographs of entry $M_{100:4560}$:N_{1000} showing hexagonally packed cylinders with a domain size of 112 nm. (a) These polymers were ordered near the air/polymer interface. The SEM micrograph of a sample that was cleaved shows the ordered cylinders near the air (the dark region on the top of (a)).

Table 2. Comparison between Domain Sizes Measured by SAXS and SEM

polymer	SAXS domain size (nm)	SEM domain size(nm)
$M_{25:3100}$:N_{250}	33	45 ± 2
$M_{25:4370}$:N_{250}	40	48 ± 7
$M_{25:6270}$:N_{250}	41	48 ± 2

Polymer Film Characterization by SAXS. Many of the comb block copolymers in Table 1 assembled into morphologies with domain sizes exceeding 90 nm, and, thus, they could not be imaged by SAXS. USAXS was another option, but due to the challenges of characterizing samples with this method and the relative ease of characterization by SEM for samples with straightforward morphologies and domain sizes exceeding 100 nm, we choose to use SEM as our primary characterization technique. Only a few polymers had domain sizes that were compatible with characterization by SAXS, so a representative group of these was analyzed by SAXS to confirm the morphologies assigned from the SEM micrographs and to provide more definitive domain sizes. These samples were the most challenging to image by SEM due to their small domain sizes. As the samples were imaged, they melted at high accelerating voltages such that high magnifications sufficient to accurately measure their domain sizes could not be used. Thus, SAXS provided a more reliable method to measure domain sizes. It is important to note that this limitation was pronounced for samples with small domain spacings, but it was not a limitation for those with larger domain spacings.

Table 2 and Figure 6 summarize our results for the three polymers that were studied. Analysis by SAXS and SEM confirmed the cylindrical morphology for these polymers; however, the domain sizes differed as expected from the difficulties of measuring domain sizes by SEM on these samples.

Tuning the Morphologies by Altering the Polymer Composition: Effect of Increasing the Molecular Weight of the Arms. Comb block copolymers are exciting new architectures to study because they allow several molecular parameters to be varied independently of each other in contrast to simpler diblock copolymers. One opportunity associated with comb block copolymers is that the composition and molecular weights of the backbone can be varied independently of the arms. Thus, two comb block copolymers may have similar compositions but very different architectures.

Here, we will describe how the morphologies and domain sizes vary for comb polymers with the same backbone polymer but with different molecular weights for the arms (Figure 7a). As the molecular weight of the arms increases, the overall composition of the comb block copolymer changes such that the morphologies proceed from lamellar to cylindrical and, finally, to disordered spheres (Table 3). This progression of phases can be rationalized by analogy to linear diblock copolymers where morphologies follow the same trend as the volume fraction of one block is increased relative to the other. In addition to changes in the morphology, the domain size increases within a morphology as the molecular weights of the arms increase. This result is easily understood as due to the increase in the overall molecular weight of the comb polymer which changes the packing constraints and interfacial curvature in the microphase-separated morphologies.

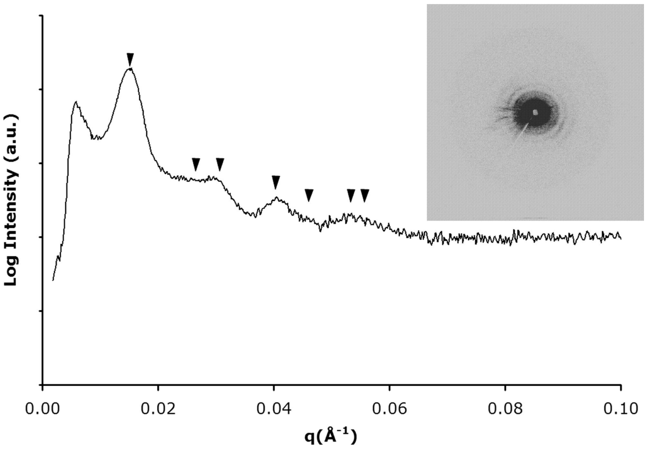

Figure 6. SAXS data for $M_{25:6270}$:N_{250} indexing consistent with hexagonally packed cylinders. The presence of the $q\sqrt{7}$ reflection confirms the morphology assigned by SEM micrographs.

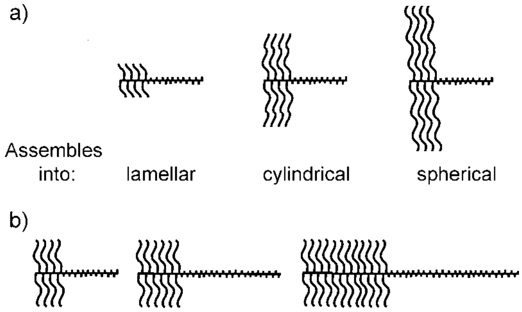

Figure 7. (a) Investigation of transition in assembled morphologies by increasing the molecular weights and volume fractions of the polymeric arms while keeping the backbone polymer constant as described in Table 3. (b) The overall composition of these polymers is constant while the molecular weights of the backbone polymers increase as described in Table 4.

Tuning the Morphologies by Altering the Polymer Composition: Effect of Altering the Degree of Polymerization of the Backbone. The ability to tune the domain size of comb block copolymer assemblies through their synthesis is an important parameter in possible future applications to the bottom-up approach of fabricating nanomaterials. It was hypothesized that the domain sizes of comb polymers could be understood by varying the overall molecular weight of the polymers, while keeping the overall volume fractions of each block constant. Thus, a series of comb polymers were synthesized where the degrees of polymerization of the backbone polymer was varied while the molecular weights of the arms and the relative composition of the backbone polymer remained nearly constant (Figure 7b). For instance, a series of polymers was studied with a ratio for the two monomers along the backbone polymer [M]/[N] = 1/10; the smaller number refers to the monomer that contains an ATRP initiator (Table 4).

In one set of polymers described in Table 4, the arms were grown to have molecular weights of ~3800 g mol^{-1} while the molecular weights of the backbone polymers were increased. The overall volume fraction of polystyrene and monomer M along the backbone were approximately 0.54 and 0.05, respectively. Each of these polymers assembled into cylindrical morphologies with increasing domain sizes as the degree of polymerization of the backbone polymer increased. In a second set of polymers, the arms were shorter (~1700 g mol^{-1}) for two comb block copolymers with backbones with degrees of polymerizations that differed by a factor of 2. These polymers assemble into lamellar morphologies with domain sizes that increased as the molecular weight of the comb polymer increased. The results from these two sets of polymers were similar to what was observed for linear block copolymers. Linear block copolymers of similar compositions assemble into the same morphology with domain sizes that increase with increasing molecular weights.

Investigation of Phase Maps. In an effort to understand the important parameters that control the self-assembly of comb

Table 3. Controlling Morphologies of Arrays by Altering Molecular Weight of the Polymeric Arm

comb block copolymer	predicted M_n for comb polymer[a] (kg mol^{-1})	percent mol/vol fraction polystyrene	percent mol/vol fraction block M	percent mol/vol fraction block N	morphology	domain size[b] (nm)
$\mathrm{M}_{200:1850}:\mathrm{N}_{2000}$	1060	62/0.37	3/0.06	35/0.57	lamellar	98 ± 10
$\mathrm{M}_{200:3240}:\mathrm{N}_{2000}$	1340	74/0.50	2/0.05	24/0.45	lamellar	114 ± 6
$\mathrm{M}_{200:3620}:\mathrm{N}_{2000}$	1410	76/0.53	2/0.05	22/0.42	cylindrical	126 ± 13
$\mathrm{M}_{200:5120}:\mathrm{N}_{2000}$	1710	82/0.62	2/0.04	16/0.34	cylindrical	137 ± 9
$\mathrm{M}_{200:6410}:\mathrm{N}_{2000}$	1970	85/0.67	1/0.03	14/0.30	spherical	

[a] Predicted from the composition of the backbone polymer and the measured molecular weight of the arms. [b] The domain size was not determined for the spherical morphology due to poor ordering.

Table 4. Controlling Domain Sizes with Increasing Backbone Polymer Molecular Weight

comb block copolymer	measured M_n for comb polymer (g mol^{-1})	percent mol/vol polystyrene	percent mol/vol block M	percent mol/vol block N	morphology	domain size (nm)
$\mathrm{M}_{25:4370}:\mathrm{N}_{250}$	212 000	79/0.58	2/0.04	19/0.38	cylinders	48 ± 7
$\mathrm{M}_{50:3530:}:\mathrm{N}_{500}$	425 000	76/0.52	2/0.05	22/0.43	cylinders	65 ± 15
$\mathrm{M}_{100:3740}:\mathrm{N}_{1000}$	510 000	77/0.54	2/0.05	21/0.41	cylinders	87 ± 12
$\mathrm{M}_{150:3750}:\mathrm{N}_{1500}$	947 000	77/0.54	2/0.05	21/0.41	cylinders	109 ± 9
$\mathrm{M}_{200:3620}:\mathrm{N}_{2000}$	1 130 000	76/0.53	2/0.05	22/0.42	cylinders	126 ± 13
$\mathrm{M}_{100:1590}:\mathrm{N}_{1000}$	410 000	58/0.33	4/0.07	38/0.60	lamellar	70 ± 4
$\mathrm{M}_{200:1850}:\mathrm{N}_{2000}$	729 000	62/0.37	3/0.06	35/0.57	lamellar	98 ± 10

block copolymers, a phase map was generated (Figure 8). Because these are new polymers that have not been thoroughly studied for their assembly in the solid state, it is important to consider what the phase map will be. The phase map will depend on the volume fraction of the densely grafted block, the degree of polymerization of the backbone, the degree of polymerization of the arms, and the Flory−Huggins interaction parameter. In this section, one phase map to order the data is shown; three other phase maps with different parameters for the *x*- and *y*-axes are supplied in the Supporting Information.

The *x*-axis is the volume fraction of the polystyrene arms plus monomer M in the backbone. Including these two volume fractions is the most realistic physical representation of this system because the polymeric arms will mostly or completely encapsulate the portion of the backbone to which they are bonded. In this representation, comb block copolymers will behave at some level like a diblock copolymer where one block is the polymer comprised of monomer N along the backbone polymer (the monomer that does not initiate the growth of the arms), and the other block is made of the arms and monomer M along the backbone. Further evidence for this model will be described in the following paragraphs.

In a typical phase diagram for linear diblock copolymers, the *y*-axis is the degree of polymerization, N, multiplied by the Flory−Huggins interaction parameter, χ.[24,25,76] When the value of χN is low, the polymer is said to be in the weak segregation limit, and when the value is high, the polymer is said to be in the strong segregation limit. The comb polymers in this study all had high degrees of polymerization and would be expected, by analogy to other polymers, to have a high value for χN and to be strongly segregated. The *y*-axis in Figure 8 is the sum of the degree of polymerization of the backbone polymer and the total sum of the degree of polymerization of the arms. Stated differently, the *y*-axis is the sum of the values of x, z, and the product of y and x as defined in Figure 1.

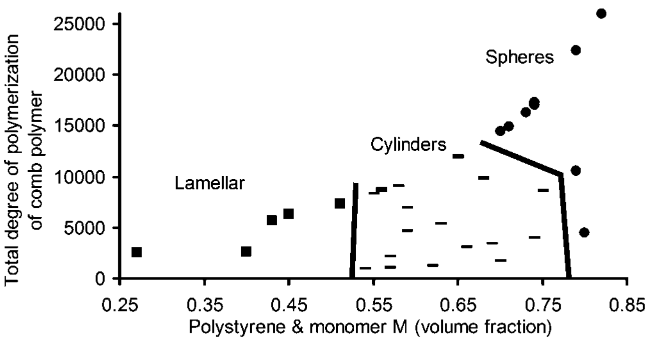

Figure 8. The *x*-axis is the volume fraction of the polystyrene arms and the monomers along the backbone to which they are bonded. The total degree of polymerization of the comb polymer (defined as the sum of the degree of polymerization of the backbone and the degrees of polymerizations of all of the arms) is plotted as the *y*-axis. The lines separating the areas rich in each morphology are drawn to aid the eye.

As expected, the phase map for comb block copolymers show important differences from phase maps for linear diblock polymers or from rod−coil block copolymers.[77−81] Linear diblock copolymers are well studied both experimentally and theoretically; their phase diagrams are well established and typically symmetric about the *x*-axis.[82−87] Rod−coil block copolymers differ from linear diblock copolymers in that one block is assumed to be shaped like a rod and the other as a random coil. The morphologies observed for rod−coil block copolymers are more numerous and complex than observed for linear diblock copolymers, which reflects the asymmetric structure of these polymers. The comb block copolymers in this study have similarities to both sets of block copolymers with important differences. For instance, comb block copolymers are conformationally and architecturally asymmetric and possess a different phase map from linear block copolymers. SEM and AFM data also show the comb block copolymers are not shaped as rod−coils, so they are not expected to share the same phase maps as rod−coils. Analogies between comb block copolymers and other polymer architectures are useful for how they might guide understanding of the morphologies, but a one-to-one mapping from comb block copolymers to other polymer architectures is not possible.

Figure 8 shows that the composition window for each morphology is shifted for the comb block copolymers compared to linear diblock copolymers. The lamellar morphology for a conformationally symmetric diblock copolymer typically extends from approximately 42% to 68% of the volume fraction of one block; yet the phase windows for our comb block copolymers clearly are shifted relative to those values. This shift is expected due to the asymmetry of these polymers and by analogy to the shift seen with block copolymers with low levels of grafts along the backbone. Another observation is that the boundary between the cylindrical and spherical morphologies is curved. Clearly, another parameter is at work, but no model of this system allowed for a clear boundary between the cylindrical and spherical morphologies. This result is not surprising as previous results with branched polymers show that they assemble into phase maps with wandering or curved boundaries.[88−93] A third observation is that morphologies seen for rod−coil polymers but not linear block copolymers (i.e., wavy lamellar, zigzag, arrowhead, and perforated lamellar) are not observed. These unobserved morphologies are understood theoretically based on the shapes of rod−coil polymers, but since our comb block copolymers did not possess a section shaped as a rod, they did not assemble into these morphologies. This observation supports the claim that comb block copolymers are close in analogy to linear diblock polymers. More theoretical and experimental work is necessary to derive a full understanding of the morphologies of these new polymers.

Conclusions

This paper represents a first step to understand and to predict the assembly of comb block copolymers in the solid state. Because these polymers are a new architecture that spans a range of domain sizes that are inaccessible by all but the highest molecular weight linear diblock copolymers, their solid-state arrays may be useful for the bottom-up approach to the fabrication of complex three-dimensional materials on a critical size scale. Before any applications can be realized, these assemblies must first be understood at a level that enables prediction of their solid-state morphology as a function of polymer composition and architecture.

Comb block copolymers have complex architectures and phase maps where analogies to linear diblock, triblock, or rod−coil polymers fail in many respects. This paper is one of the first to examine this new polymer architecture to learn how their structures correlate with observed domain sizes and morphologies in the solid state. Toward this end, a series of four phase maps were generated to provide a basis for predicting morphologies based on compositions. Interestingly, these phase maps that showed regions rich in each morphology; however, overlap was observed between the cylindrical and spherical morphologies. The reasons for the overlap are not clear and point to future directions where theoretical modeling will be useful. The morphologies that were observed were directly comparable to those seen for linear diblock copolymers rather than triblock or rod−coil polymers.

A series of trends between molecular weights and domain sizes demonstrate how the molecular weights and compositions of the arms and backbone polymers affect domain sizes. These domain sizes are much larger than those seen for all but the highest molecular weight linear block copolymers and made the arrays optically colored. Because of this, these arrays may have real applications due to their large sizes and order on a size scale that is interesting for optics. In addition, the composition of the backbone polymer or the arms can be easily varied to allow for a wide range of different functional groups to be designed into these polymers that will lead to functional arrays in the solid state. In future work, we will study some of these opportunities to assemble more functional, complex arrays from comb block copolymers.

Acknowledgment. N.B. thanks the National Science Foundation (DMR 0734158), the Roy J. Carver Charitable Trust, and the Research Corporation for their generous financial support. A.T. thanks the University of Iowa for financial support. M.M. thanks the NSF NSEC/MRSEC soft matter characterization facility at the University of Wisconsin.

Supporting Information Available: Details of the characterization of the backbone polymers and scanning electron micrographs of the arrays of polymers. This material is available free of charge via the Internet at http://pubs.acs.org.

References and Notes

(1) Hillmyer, M. A. *J. Polym. Sci., Part B: Polym. Phys.* **2007**, *45*, 3249–3251.
(2) Bates, F. S.; Fredrickson, G. H. *Phys. Today* **1999**, *52*, 32–38.
(3) Lipic, P. M.; Bates, F. S.; Hillmyer, M. A. *J. Am. Chem. Soc.* **1998**, *120*, 8963–8970.
(4) Ikkala, O.; ten Brinke, G. *Science* **2002**, *295*, 2407–2409.
(5) Stoykovich, M. P.; Muller, M.; Kim, S. O.; Solak, H. H.; Edwards, E. W.; de Pablo, J. J.; Nealey, P. F. *Science* **2005**, *308*, 1442–1446.
(6) Kim, S. O.; Solak, H. H.; Stoykovich, M. P.; Ferrier, N. J.; de Pablo, J. J.; Nealey, P. F. *Nature (London)* **2003**, *424*, 411–414.
(7) Lodge, T. P. *Macromol. Chem. Phys.* **2003**, *204*, 265–273.
(8) Xiao, S.; Yang, X.; Edwards, E. W.; La, Y.-H.; Nealey, P. F. *Nanotechnology* **2005**, *16*, 324–329.
(9) Hawker, C. J.; Russell, T. P. *MRS Bull.* **2005**, *30*, 952–966.
(10) Hamley, I. W. *Nanotechnology* **2003**, *14*, R39−R54.
(11) Miller, A. C.; Bennett, R. D.; Hammond, P. T.; Irvine, D. J.; Cohen, R. E. *Macromolecules* **2008**, *41*, 17391744\.
(12) Hameed, N.; Guo, Q. *Polymer* **2008**, *49*, 922–933.
(13) Schmidt, K.; Schoberth, H. G.; Ruppel, M.; Zettl, H.; Haensel, H.; Weiss, T. M.; Urban, V.; Krausch, G.; Boeker, A. *Nat. Mater.* **2008**, *7*, 142–145.
(14) Baralia, G. G.; Filiatre, C.; Nysten, B.; Jonas, A. M. *Adv. Mater. (Weinheim, Ger.)* **2007**, *19*, 4453–4459.
(15) Guo, F.; Jankova, K.; Schulte, L.; Vigild, M. E.; Ndoni, S. *Macromolecules* **2008**, *41*, 1486–1493.
(16) Gong, Y.; Joo, W.; Kim, Y.; Kim, J. K. *Chem. Mater.* **2008**, *20*, 1203–1205.
(17) Fahmi, A.; Pietsch, T.; Gindy, N. *Macromol. Rapid Commun.* **2007**, *28*, 2300–2305.
(18) Lanson, D.; Schappacher, M.; Borsali, R.; Deffieux, A. *Macromolecules* **2007**, *40*, 9503–9509.
(19) ten Brinke, G.; Ruokolainen, J.; Ikkala, O. *Adv. Polym. Sci.* **2007**, *207*, 113–177.
(20) Matsushita, Y. *Macromolecules* **2007**, *40*, 771–776.
(21) Huck, W. T. S. *Chem. Commun. (Cambridge, U.K.)* **2005**, 4143–4148.
(22) Hamley, I. W. *Nanotechnology* **2003**, *14*, R39−R54.
(23) Krausch, G.; Magerle, R. *Adv. Mater. (Weinheim, Ger.)* **2002**, *14*, 1579–1583.
(24) Bates, F. S.; Fredrickson, G. H. *Annu. Rev. Phys. Chem.* **1990**, *41*, 525–557.
(25) Fredrickson, G. H.; Bates, F. S. *Annu. Rev. Mater. Sci.* **1996**, *26*, 501–550.
(26) Hartikainen, J.; Lahtinen, M.; Torkkeli, M.; Serimaa, R.; Valkonen, J.; Rissanen, K.; Ikkala, O. *Macromolecules* **2001**, *34*, 7789–7795.
(27) Ikkala, O.; ten Brinke, G. *Chem. Commun.* **2004**, 2131–2137.
(28) Kosonen, H.; Valkama, S.; Ruokolainen, J.; Torkkeli, M.; Serimaa, R.; ten Brinke, G.; Ikkala, O. *Eur. Phys. J. E* **2003**, *10*, 69–75.
(29) Ten Brinke, G.; Ikkala, O. *Chem. Rec.* **2004**, *4*, 219–230.
(30) Edrington, A. C.; Urbas, A. M.; DeRege, P.; Chem, C. X.; Swager, T. M.; Hadijchristidis, N.; Xenidou, M.; Fetters, L. J.; Joannopoulos, J. D.; Fink, Y.; Thomas, E. L. *Adv. Mater.* **2001**, *13*, 421–425.
(31) Fink, Y.; Winn, J. N.; Fan, S.; Chen, C.; Michel, J.; Joannopoulos, J. D.; Thomas, E. L. *Science* **1998**, *282*, 1679–1682.
(32) Deng, T.; Chen, C.; Honeker, C.; Thomas, E. L. *Polymer* **2003**, *44*, 6549–6553.
(33) Maldovan, M.; Thomas, E. L. *Nat. Mater.* **2004**, *3*, 593–600.
(34) Kamp, M.; Happ, T.; Mahnkopf, S.; Forchel, A.; Anand, S.; Duan, G.-H. *Photonic Cryst.* **2004**, 329–346.
(35) Beers, K. L.; Woodworth, B.; Matyjaszewski, K. *J. Chem. Educ.* **2001**, *78*, 544–547.
(36) Matyjaszewski, K.; Xia, J. *Chem. Rev.* **2001**, *101*, 2921–2990.
(37) Trnka, T. M.; Grubbs, R. H. *Acc. Chem. Res.* **2001**, *34*, 18–29.
(38) Sanford, M. S.; Love, J. A.; Grubbs, R. H. *J. Am. Chem. Soc.* **2001**, *123*, 6543–6554.
(39) Sanford, M. S.; Henling, L. M.; Day, M. W.; Grubbs, R. H. *Angew. Chem., Int. Ed.* **2000**, *39*, 3451–3453.
(40) Schrock, R. R. *Tetrahedron* **1999**, *55*, 8141–8153.
(41) Kricheldorf, H. R.; Kreiser-Saunders, I.; Boettcher, C. *Polymer* **1995**, *36*, 1253–1259.
(42) Koutalas, G.; Iatrou, H.; Lohse, D. J.; Hadjichristidis, N. *Macromolecules* **2005**, *38*, 4996–5001.
(43) Kolb, H. C.; Finn, M. G.; Sharpless, K. B. *Angew. Chem., Int. Ed.* **2001**, *40*, 2004–2021.
(44) Denesyuk, N. A. *Phys. Rev. E* **2003**, *68*, 031803/1–031803/11.
(45) Corbin, P. S.; Webb, M. P.; McAlvin, J. E.; Fraser, C. L. *Biomacromolecules* **2001**, *2*, 223–232.
(46) Matyjaszewski, K. *Polym. Mater. Sci. Eng.* **2001**, *84*, 363–364.
(47) Quinn, J. F.; Chaplin, R. P.; Davis, T. P. *J. Polym. Sci., Part A: Polym. Chem.* **2002**, *40*, 2956–2966.
(48) Shi, P.-J.; Li, Y.-G.; Pan, C.-Y. *Eur. Polym. J.* **2004**, *40*, 1283–1290.
(49) Tao, L.; Luan, B.; Pan, C.-Y. *Polymer* **2003**, *44*, 1013–1020.

(50) Yoon, J.; Mathers, R. T.; Coates, G. W.; Thomas, E. L. *Macromolecules* **2006**, *39*, 1913–1919.

(51) Runge, M. B.; Bowden, N. B. *J. Am. Chem. Soc.* **2007**, *129*, 10551–1060.

(52) Burchard, W.; Schmidt, M.; Stockmayer, W. H. *Macromolecules* **1980**, *13*, 1265–1272.

(53) Daniels, D. R.; McLeish, T. C. B.; Crosby, B. J.; Young, R. N.; Fernyhough, C. M. *Macromolecules* **2001**, *34*, 7025–7033.

(54) Dekmezian, A. H.; Weng, W.; Garcia-Franco, C. A.; Markel, E. J. *Polymer* **2004**, *45*, 5635–5640.

(55) Inkson, N. J.; Graham, R. S.; McLeish, T. C. B.; Groves, D. J.; Fernyhough, C. M. *Macromolecules* **2006**, *39*, 4217–4227.

(56) Ito, K.; Tomi, Y.; Kawaguchi, S. *Macromolecules* **1992**, *25*, 1534–1538.

(57) Kapnistos, M.; Vlassopoulos, D.; Roovers, J.; Leal, L. G. *Macromolecules* **2005**, *38*, 7852–7862.

(58) Meuhlebach, A.; Rime, F. *J. Polym. Sci., Part A: Polym. Chem.* **2003**, *41*, 3425–3439.

(59) Mijovic, J.; Sun, M.; Pejanovic, S.; Mays, J. W. *Macromolecules* **2003**, *36*, 7640–7651.

(60) Nakamura, Y.; Norisuye, T. *Polym. J.* **2001**, *33*, 874–878.

(61) Potemkin, I. I.; Khokhlov, A. R.; Prokhorova, S.; Sheiko, S. S.; Moeller, M.; Beers, K. L.; Matyjaszewski, K. *Macromolecules* **2004**, *37*, 3918–3923.

(62) Runge, M. B.; Dutta, S.; Bowden, N. B. *Macromolecules* **2006**, *39*, 498–508.

(63) Snyder, J. F.; Hutchison, J. C.; Ratner, M. A.; Shriver, D. F. *Chem. Mater.* **2003**, *15*, 4223–4230.

(64) Subbotin, A.; Saariaho, M.; Ikkala, O.; ten Brinke, G. *Macromolecules* **2000**, *33*, 3447–3452.

(65) Tsukahara, Y.; Kohjiya, S.; Tsutsumi, K.; Okamoto, Y. *Macromolecules* **1994**, *27*, 1662–1664.

(66) Tsoukatos, T.; Pispas, S.; Hadjichristidis, N. *Macromolecules* **2000**, *33*, 9504–9511.

(67) Valkama, S.; Lehtonen, O.; Lappalainen, K.; Kosonen, H.; Castro, P.; Repo, T.; Torkkeli, M.; Serimaa, R.; ten Brinke, G.; Leskelae, M.; Ikkala, O. *Macromol. Rapid Commun.* **2003**, *24*, 556–560.

(68) Hadijchristidis, N.; Pitsikalis, M.; Iatrou, H.; Pispas, S. *Macromol. Rapid Commun.* **2003**, *24*, 979–1013.

(69) Wang, R.; Jiang, Z.; Hu, J. *Polymer* **2005**, *46*, 6201–6207.

(70) Saariaho, M.; Subbotin, A.; Szleifer, I.; Ikkala, O.; ten Brinke, G. *Macromolecules* **1999**, *32*, 4439–4443.

(71) Sheng, Y.-J.; Cheng, K.-L.; Ho, C.-C. *J. Chem. Phys.* **2004**, *121*, 1962–1968.

(72) *Light Scattering from Polymer Solutions*; Huglin, M. B., Ed.; Academic Press: New York, 1972.

(73) Berne, B. J.; Pecora, R. *Dynamic Light Scattering: With Applications to Chemistry, Biology, and Physics*; Dover Publications: Mineola, NY, 2000.

(74) Rodriguez, F. *Principles of Polymer Systems*; Taylor and Francis: Philadelphia, PA, 1996.

(75) Runge, M. B.; Dutta, S.; Bowden, N. B. *Polym. Prepr.* **2005**, *92*, 5–6.

(76) Flory, P. J. *Principles of Polymer Chemistry*; Cornell University Press: Ithaca, NY, 1953.

(77) Ye, X.-G.; Sun, Z.-Y.; Li, H.-F.; Tong, Z. *J. Chem. Phys.* **2008**, *128*−1/5.

(78) Stepanyan, R.; Subbotin, A.; ten Brinke, G. *Macromolecules* **2002**, *35*, 5640–5648.

(79) Foster, D. P.; Jasnow, D.; Balazs, A. C. *Macromolecules* **1995**, *28*, 3450–3462.

(80) Khalatur, P. G.; Khokhlov, A. R. *J. Chem. Phys.* **2000**, *112*, 4849–4861.

(81) Wang, R.; Jiang, Z.; Hu, J. *Polymer* **2005**, *45*, 6201–6207.

(82) Shah, M.; Pryamitsyn, V.; Ganesan, V. *Macromolecules* **2008**, *41*, 218–229.

(83) Hernandez-Jimenez, M., Jr. *Soft Matter* **2007**, *23*, 31–42.

(84) Olsen, B. D.; Segalman, R. A. *Macromolecules* **2007**, *40*, 6922–6929.

(85) Olsen, B. D.; Li, X.; Wang, J.; Segalman, R. A. *Macromolecules* **2007**, *40*, 3287–3295.

(86) Sary, N.; Rubatat, L.; Brochon, C.; Hadziioannou, G.; Ruokolainen, J.; Mezzenga, R. *Macromolecules* **2007**, *40*, 6990–6997.

(87) Olsen, B. D.; Alcazar, D.; Krikorian, V.; Toney, M. F.; Thomas, E. L.; Segalman, R. A. *Macromolecules* **2008**, *41*, 58–66.

(88) Matsen, M. W. *J. Chem. Phys.* **2000**, *113*, 5539–5544.

(89) Matsen, M. W.; Gardiner, J. M. *J. Chem. Phys.* **2000**, *113*, 1673–1676.

(90) Grason, G. M.; Kamien, R. D. *Macromolecules* **2004**, *37*, 7371–7380.

(91) Pochan, D. J.; Gido, S. P.; Pispas, S.; Mays, J. W. *Macromolecules* **1996**, *29*, 5099–5105.

(92) Pochan, D. J.; Gido, S. P.; Pispas, S.; Mays, J. W.; Ryan, A. J.; Fairclough, J. P. A.; Hamley, I. W.; Terrill, N. J. *Macromolecules* **1996**, *29*, 5091–5098.

(93) Gido, S. P.; Lee, C.; Pochan, D. J.; Pispas, S.; Mays, J. W.; Hadjichristidis, N. *Macromolecules* **1996**, *29*, 7022–7028.

MA8009323